

Low-Valency Carbomolybdates and -tungstates

Enkhtsetseg Dashjav, Guido Kreiner, Frank R. Wagner, Walter Schnelle, and Rüdiger Kniep

Recently, we have introduced criteria for carbometalates (see “*Ternary Carbides from the Point of View of Carbometalates*”) by extending the concept of complex anions from fluoro-, oxo-, nitrido- to carbometalates [1]. The concept has successfully been applied to a number of novel low-valency carbomolybdates and carbotungstates [1-5]: $RE_2[MoC_2]$ ($RE = Pr, Nd$), $RE_2[WC_2]$ ($RE = Ce, Pr, Nd$) and $RE_2[Mo_2C_3]$ ($RE = Ce, Pr, Gd - Dy$). The oxidation state of the transition metal T is +2 in case of the general formula $RE_2[TC_2]$ while it yields +3 for $RE_2[Mo_2C_3]$ compounds. For comparison, the oxidation state of the transition metals in all known nitridomolybdates and -tungstates is +6 (e.g., $Li_6[MoN_4]$ or $Ba_3[TN_4]$ ($T = Mo, W$) [7,8]).

All compounds were obtained by arc-melting mixtures of the elements in stoichiometric amounts and subsequent heat treatment at ca 1700 K and were characterized by chemical analyses, X-ray diffraction techniques and metallographic examination of the microstructures.

$RE_2[MoC_2]$ ($RE = Pr, Nd$), $RE_2[WC_2]$ ($RE = Ce, Pr, Nd$) crystallize isotypically in a novel structure type ($Pr_2[MoC_2]$ type, tetragonal, $P4_2/mnm$, $Z = 4$). Selected crystallographic data for the various compounds are listed in Tab. 1.

The crystal structures consist of layered polyanions ${}^2_2[(TC_{4/2})^6-]$ (Fig. 1) of distorted vertex and edge sharing TC_4 tetrahedra. The rare earth metals are also in a distorted tetrahedral coordination by carbon. The metal atoms form a distorted *bcc* arrangement ($MoSi_2$ motif) with carbon atoms occupying a fraction of the octahedral voids (Fig. 2). The physical properties show metallic behavior and fully local-

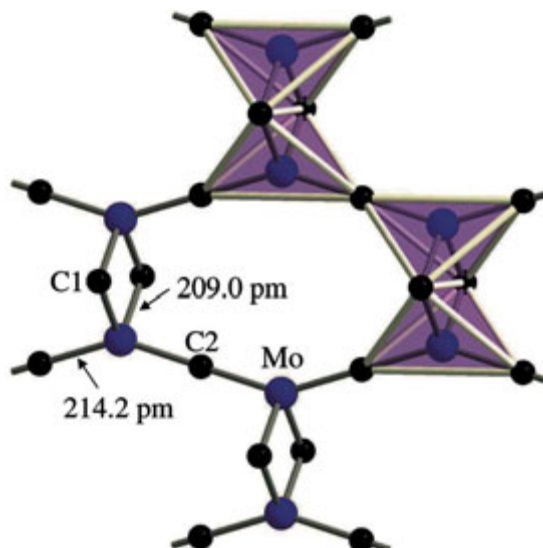


Fig. 1: The crystal structure of $Pr_2[MoC_2]$. The layered polyanion ${}^2_2[(Mo_2C_{4/2})^6-]$ consists of distorted vertex- and edge-sharing MoC_4 tetrahedra.

ized magnetic $4f$ -moments except for the Ce compound, thus the presence of Pr^{3+} and Nd^{3+} species. A detailed bonding analysis using both the electron localization function (ELF) and the COHP method justifies an interpretation as carbometalates(II). ELF diagrams have been calculated for $La_2[MoC_2]$ as a model compound. The ELF shows for all Mo–C contacts characteristic local maxima along the connecting line of the atoms (Fig. 3). In addition, the atom type C1 (bridging ligand) reveals yet another maximum which is oriented towards the void of the neighboring RE_4 tetrahedron (Fig. 2). The latter is interpreted as a lone pair. In addition to the strong Mo–C interactions of covalent nature, the ELF dia-

Compound	a (pm)	c (pm)	V/Z ($10^6 pm^3$)	RE^{n+}	r (pm)	Ref.
$Pr_2[MoC_2]$	581.3	1032.5	174.5	Pr^{3+}	106	[1]
$Nd_2[MoC_2]$	580.4	1024.8	172.6	Nd^{3+}	104	[2]
$Pr_2[WC_2]$	579.5	1035.7	173.9	Pr^{3+}	106	[2]
$Nd_2[WC_2]$	578.9	1027.8	172.3	Nd^{3+}	104	[2]
$Ce_2[WC_2]$	570.7	1038.8	169.2	Ce^{4+}	94	[2]

Tab. 1. Unit cell parameters and unit cell volume per formula unit of carbomolybdates(II) and -tungstates(II) $RE_2[TC_2]$. The ionic radii of the rare earth cations are also given.

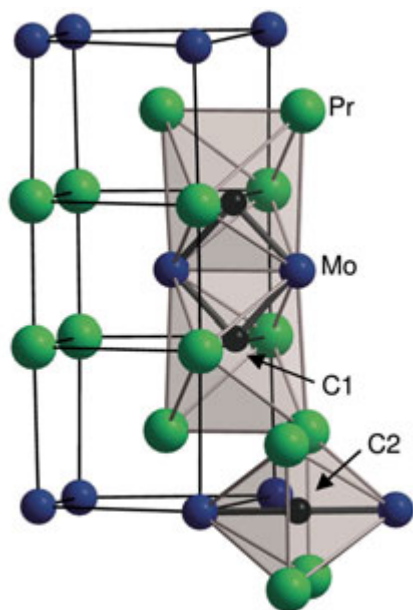


Fig. 2: The crystal structure of $\text{Pr}_2[\text{MoC}_2]$. The metal atoms Pr and Mo form a distorted bcc arrangement (MoSi_2 motif) with carbon atoms occupying a fraction of the octahedral voids.

gram supports much weaker metal–metal interactions of complex nature as illustrated by the green basins in the ELF diagram. Thus, it appears that the ionic formula $(\text{RE}^{3+})_2[\text{T}^{2+}(\text{C}^4)_2]$ is appropriate to describe the respective oxidation states for compounds crystallizing in the $\text{Pr}_2[\text{MoC}_2]$ type with the exception of the Ce compound.

In case of $\text{RE}_2[\text{Mo}_2\text{C}_3]$ as general formula two different crystal structure types have been observed. Carbomolybdates containing the rare earth metals $\text{RE} = \text{Ce}, \text{Gd} - \text{Er}$ crystallize in the $\text{Er}_2[\text{Mo}_2\text{C}_3]$ type [2] while the praseodymium containing compound crystallizes in a novel structure type. Selected crystallographic data for the various compounds are listed in Tab. 2.

Compound	<i>a</i> (pm)	<i>b</i> (pm)	<i>c</i> (pm)	β (°)	<i>V</i> / <i>Z</i> (10^6 pm^3)	RE^{n+}	<i>r</i> (pm)	Ref.
$\text{Pr}_2[\text{Mo}_2\text{C}_3]^{\text{a}}$	598.0	665.2	1185.6	111.6	109.6	Pr^{3+}	106	[1]
$\text{Gd}_2[\text{Mo}_2\text{C}_3]^{\text{b}}$	1187.0	335.8	575.6	113.1	105.5	Gd^{3+}	97	[4]
$\text{Ce}_2[\text{Mo}_2\text{C}_3]^{\text{b}}$	1203.2	333.7	574.7	114.0	105.4	Ce^{4+}	94	[5]
$\text{Tb}_2[\text{Mo}_2\text{C}_3]^{\text{b}}$	1178.5	333.8	571.8	112.6	103.9	Tb^{3+}	93	[5]
$\text{Dy}_2[\text{Mo}_2\text{C}_3]^{\text{b}}$	1172.4	333.4	570.0	112.1	103.2	Dy^{3+}	91	[5]
$\text{Ho}_2[\text{Mo}_2\text{C}_3]^{\text{b}}$	1161.6	332.1	566.1	111.6	101.5	Ho^{3+}	89	[6]
$\text{Er}_2[\text{Mo}_2\text{C}_3]^{\text{b}}$	1155.9	330.9	563.7	111.3	100.5	Er^{3+}	88	[6]

a) $\text{Pr}_2[\text{Mo}_2\text{C}_3]$ type; b) $\text{Er}_2[\text{Mo}_2\text{C}_3]$ type

Tab. 2. Unit cell parameters and unit cell volume per formula unit for the carbomolybdates(III) $\text{RE}_2[\text{Mo}_2\text{C}_3]$. The ionic radii of the rare earth cations are also given.

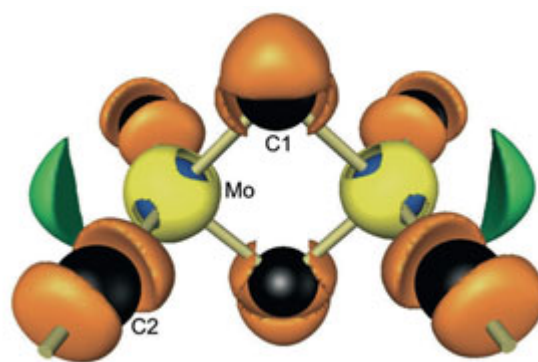


Fig. 3: The crystal structure of $\text{Pr}_2[\text{MoC}_2]$. ELF diagram for $[\text{Mo}_2\text{C}_{12}\text{C}_{24/2}]$ units. The Mo–C contacts show characteristic local maxima along the connecting line of the atoms (orange domains with $\eta = 0.78$). In addition, the bridging ligand reveals another maximum which is interpreted as a lone pair. Green domains with $\eta = 0.43$ indicate multicenter metal–metal interactions.

The crystal structure of $\text{Pr}_2[\text{Mo}_2\text{C}_3]$ ($Z = 4$, monoclinic, $P2_1/c$) represents a novel structure type containing a three dimensional polyanion ${}^3_2[(\text{Mo}_2\text{C}_3)^6]$ with molybdenum(III) in a distorted tetrahedral coordination by carbo-ligands. Tetrameric building-blocks Mo_4C_{10} of edge sharing MoC_4 tetrahedra (Fig. 4) are arranged to form layers running parallel (100). The layers are interconnected along [100] by sharing common apices of the MoC_4 tetrahedra (Fig. 5). The coordination polyhedra around praseodymium represent distorted (PrC_5)-arrangements (mono capped tetrahedra and square pyramids). The metal atoms together form a distorted motif of a body centred cubic arrangement (Fig. 6) with the carbo-ligands occupying a part of the octahedral voids. The physical properties of the new ternary compound are consistent with metallic behavior with localized magnetic $4f$ -moments in agreement with the presence of Pr^{3+} species. A detailed analy-

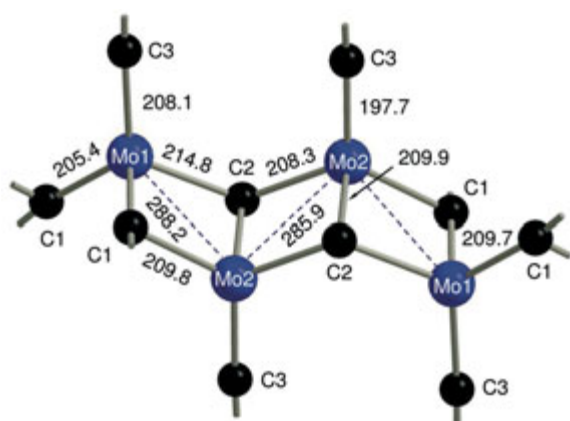


Fig. 4: The crystal structure of $\text{Pr}_2[\text{Mo}_2\text{C}_3]$. The tetrameric building-block, Mo_4C_{10} , consists of four edge-sharing MoC_4 -tetrahedra.

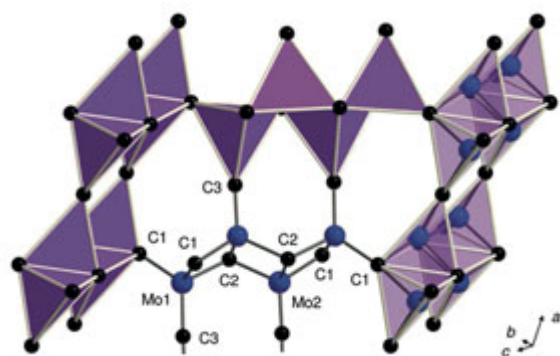


Fig. 5: The crystal structure of $\text{Pr}_2[\text{Mo}_2\text{C}_3]$. The Mo_4C_{10} units form layers running parallel to (100) . The layers are then interconnected along $[100]$ by sharing common apices of the MoC_4 tetrahedra.

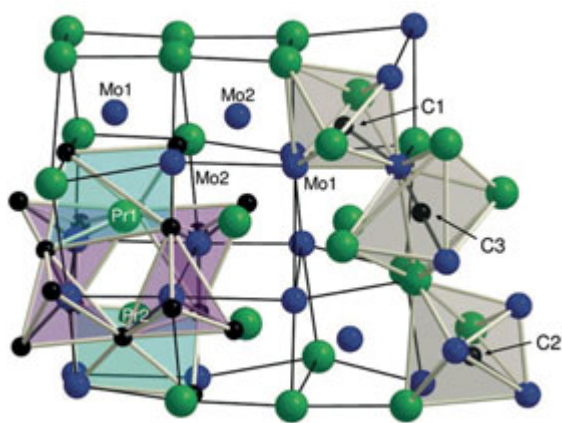


Fig. 6: The crystal structure of $\text{Pr}_2[\text{Mo}_2\text{C}_3]$. The metal atoms Pr and Mo form a bcc arrangement with the carbo-ligands partly occupying the octahedral voids.

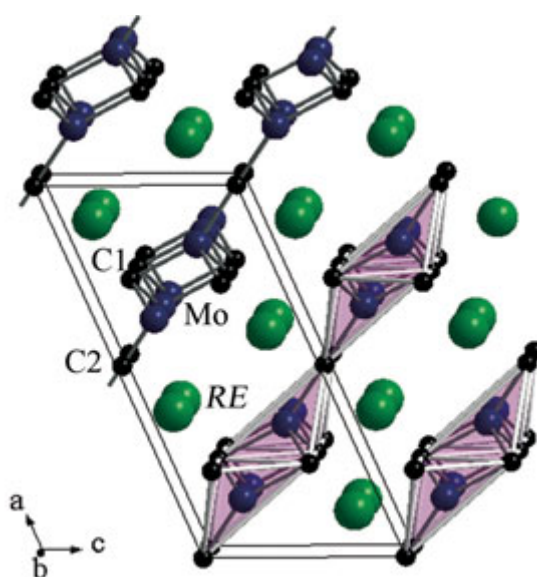


Fig. 7: The $\text{Er}_2[\text{Mo}_2\text{C}_3]$ structure type. The crystal structure consists of a stacking of ${}^2_2[\text{Mo}_2\text{C}_3]^{6-}$ layers with rare earth atoms ($\text{RE} = \text{Ce}, \text{Gd} - \text{Er}$) in between. The layers are formed by infinite chains of edge connected, distorted MoC_4 tetrahedra which are then vertex connected via the remaining apices to form two-dimensional layers.

sis of the chemical bonding situation using both the density of states (DOS) and the COHP method justifies again the interpretation of the title compound as a carbomolybdate(III).

In case of the $\text{Er}_2[\text{Mo}_2\text{C}_3]$ type ($Z = 2$, monoclinic, $C2/m$), the crystal structures consist of stacked ${}^2_2[\text{Mo}_2\text{C}_3]^{6-}$ layers with $\text{RE} = \text{Ce}, \text{Gd} - \text{Er}$ with rare-earth cations in between. The polyanions form infinite chains via edge-sharing ($\text{C1} \cdots \text{C1}$) of distorted MoC_4 tetrahedra. The latter are vertex-connected via the remaining two apices (C2) to form two-dimensional layers (Fig. 7). The metal atoms form a distorted bcc arrangement (Fig. 8) with the carbon atoms occupying a fraction of the octahedral voids. The carbon atoms are connected to three (C1) and two (C2) Mo atoms, respectively. The coordination polyhedron around the RE atoms represents a REC_5 square pyramid with RE being slightly shifted out of the square plane. The electrical resistivities $\rho(T)$ show linear temperature dependences for $T > 80$ K indicating a metallic conduction behavior. The measured values of $\rho(T)$ at 300 K vary between $60 \mu\Omega\text{cm}$ and $140 \mu\Omega\text{cm}$ for the compact bulk samples. The magnetic susceptibilities (Fig. 9) of the $\text{RE}_2[\text{Mo}_2\text{C}_3]$ compounds are all quite different. However, with the exception of the Ce compound, the obtained values of μ_{eff} are close to those for the

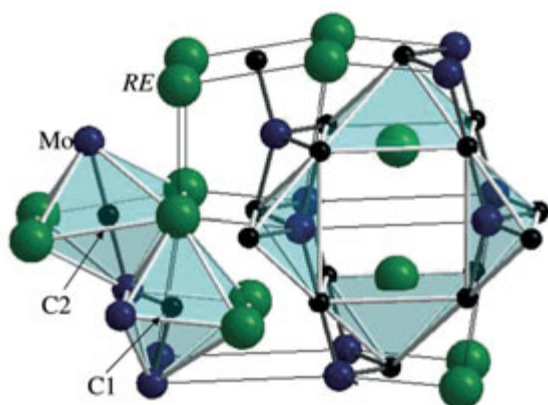


Fig. 8: The $Er_2[Mo_2C_3]$ structure type. The metal atoms RE and Mo form a bcc arrangement with the carbo-ligands partly occupying the octahedral voids.

respective free RE^{3+} ions and the magnetic moments order antiferromagnetically at lower temperatures. For example, the effective moment of the Gd compound is $8.02 \mu_B$ per Gd atom, which is in agreement with the theoretical value of $7.94 \mu_B$ for the Gd^{3+} ion. In analogy to the carbometalates(II), the ionic limit $(RE^{3+})_2[(Mo^{3+})_2(C^{4-})_3]$ is appropriate to describe the oxidation states of the corresponding species, again with the exception of the Ce compound.

The special position of the Ce compounds $Ce_2[WC_2]$ and $Ce_2[Mo_2C_3]$ is demonstrated by their unusual small unit cell volume per formula unit assuming an oxidation state of +3 for the RE ions ($r = 107$ pm for Ce^{3+}). In case of Ce^{3+} compounds the expected unit cell volume per formula unit should be close to those of the Pr compounds. However, for $Ce_2[Mo_2C_3]$ the volume is close to that of the Gd compound. Magnetic moments are compatible with a $4f^0$ configuration instead of the expected $4f^1$ configuration for Ce^{3+} species. In the same way, the electronic specific heat coefficient γ of $Ce_2[Mo_2C_3]$ extrapolated from $c_p(T)$ is $104 - 110 \text{ mJ mol}^{-1} \text{ K}^{-2}$ is clearly enhanced which is typical for a valence fluctuating Ce compound close to Ce^{4+} . Electronic band structure calculations indicate that Ce centered electrons ($Ce^{4+} \cdot e^-$) have substantial d character and are delocalized to form partial Ce–Ce bonds instead of being local-

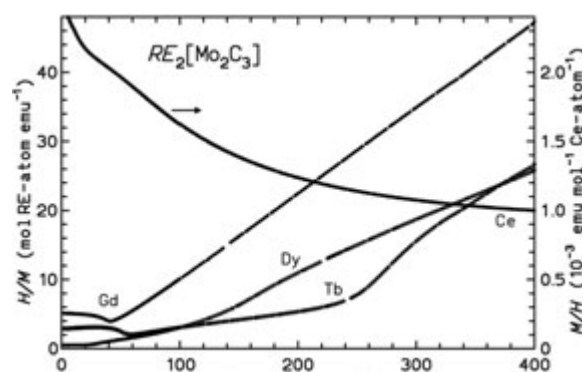


Fig. 9: Inverse magnetic susceptibility H/M versus temperature T for samples of $RE_2[Mo_2C_3]$ with $RE = Gd, Tb, Dy$ (left scale) and magnetic susceptibility of $Ce_2[Mo_2C_3]$ (right scale).

ized in Ce centered f states. Therefore, the appropriate ionic formulae are $((Ce^{4+} \cdot e^-)^{3+})_2[W^{2+}(C^{4-})_2]$ and $((Ce^{4+} \cdot e^-)^{3+})_2[(Mo^{3+})_2(C^{4-})_3]$ in agreement with the concept of carbometalates. The situation resembles that of the compound CeN [9] which is non-magnetic despite the fact that it contains cerium with the oxidation state +3.

References

- [1] E. Dashjav, G. Kreiner, W. Schnelle, F. R. Wagner, and R. Kniep, *Z. Anorg. Allg. Chem.* **630** (2004) 689.
- [2] E. Dashjav, G. Kreiner, W. Schnelle, F. R. Wagner, and R. Kniep, 12. Vortragstagung der GDCh, Marburg, Germany, (2004).
- [3] E. Dashjav, G. Kreiner, W. Schnelle, F. R. Wagner, and R. Kniep, *Z. Anorg. Allg. Chem.* **630** (2004) 227.
- [4] E. Dashjav, G. Kreiner, W. Schnelle, and R. Kniep, *Z. Krist. NCS* **2** (2005) 131.
- [5] E. Dashjav, G. Kreiner, W. Schnelle, F. R. Wagner, and R. Kniep, *Z. Kristallogr. Suppl.* **22** (2005) 144.
- [6] R. Reehuis, M. Gerdes, W. Jeitschko, B. Ouladdiaf, and N. Stüsser, *J. Mag. Magn. Mater.* **195** (1999) 657.
- [7] A. Gudat, S. Haag, R. Kniep, and A. Rabenau, *Z. Naturforsch.* **45b** (1990) 111.
- [8] A. Gudat, P. Höhn, R. Kniep, and A. Rabenau, *Z. Naturforsch.* **46b** (1991) 566.
- [9] G. A. Landrum, R. Dronskowski, R. Niewa, and F. J. DiSalvo, *Chem. Eur. J.* **5** (1999) 515.